Magneto-optical evidence of many-body effects in a spin-polarized two-dimensional electron gas

A. Lemaître, C. Testelin, and C. Rigaux
Groupe de Physique des Solides, Universités Paris 6 et 7, 2, place Jussieu, 75231 Paris Cedex 05, France

T. Wojtowicz and G. Karczewski
Institute of Physics, Polish Academy of Sciences, Al. Lotników 32/46, 02-668 Warszawa, Poland
(Received 29 October 1999; revised manuscript received 17 March 2000)

Modulation-doped $Cd_xMn_{1-x}Te/Cd_yMg_{1-y}Te$ quantum wells are studied at 1.7 K by magnetoabsorption experiments performed near the fundamental heavy-hole–electron (HH_1-E_1) transition. In the investigated range of Mn content ($x \approx 0.02$) and electron concentration [$n_e \approx (2-3)\times 10^{11}$ cm^{-2}], the two-dimensional electron gas is fully spin-polarized at magnetic fields as low as $H = 1.5$ T. The interband optical spectra exhibit unusual magnetic field dependence resulting from electron-hole interactions and phase-space-filling effects. An additional enhancement of the spin splitting of Landau levels found in this study is attributed to the electron-exchange interaction. A simplified theoretical model including the exchange energy and the electron-hole interaction provides a coherent quantitative description of the overall experimental features.

I. INTRODUCTION

The presence of a two-dimensional electron gas (2DEG) significantly affects optical properties of quantum well (QW) structures. Recently, the formation of exciton-electron complexes (trions) has been observed for QW's with a moderate 2DEG concentration, of the order of 10^{10} cm^{-2}.[1,2] New processes of optical excitation (the exciton-cyclotron resonance[3,4]) and recombination (the Fermi surface shake-up process[5]) have been seen in external magnetic fields. With increasing electron density both the exciton binding energy and the oscillator strength of excitonic transitions decrease, which is commonly attributed to many-body effects such as screening, phase-space filling, and exchange interactions.[6–11]

Due to the large effective Rydberg in II-VI compounds (10 meV in CdTe as compared to 4.3 meV in GaAs), modulation-doped quantum wells (MDQW) formed from CdTe are of particular interest to study the influence of electrons on optical spectra of low-dimensional structures. The importance of carrier-exciton interactions was clearly demonstrated by the observation of negatively (or positively) charged excitons in n- (or p-) doped CdTe and $Cd_xMn_{1-x}Te$ QW.[1,12,13] The evolution of absorption spectra with the electron concentration n_e was recently reported for CdTe MDQW's:[14] the exciton line, which dominates the spectrum at a very low concentration, shifts to higher energies with increasing n_e and subsequently disappears for $n_e \approx (2-3)\times 10^{11}$ cm^{-2}. The lowest-energy excitation, which is due to the negatively charged exciton, X^-, remains quasistable with the electron density and at high n_e (3×10^{11} cm^{-2}) it evolves into a broad band (associated with a ''Fermi edge singularity'' in Refs. 1 and 14). A similar behavior of the trion energy has been found in n- and p-doped $Cd_xMn_{1-x}Te$ MDQWs.[12,13] In the presence of magnetic fields the broad band splits into transitions between the electron and hole Landau levels.[15–17]

In this paper, we report experimental evidence of the influence of many-body effects in the two-dimensional electron gas on magneto-optical spectra of MDQW's. The magnetotransmission studies were carried out in a MDQW (n-type doped) made of a diluted magnetic semiconductor (DMS) $Cd_{1-x}Mn_xTe$ surrounded by nonmagnetic barriers $Cd_{1-y}Mg_yTe$. Within the chosen concentration range [$n_e \approx (2-3)\times 10^{11}$ cm^{-2}], the Coulomb interaction is considerably reduced and the magneto-optical spectra near the $HH_1 \rightarrow E_1$ fundamental transition are dominated by the Landau quantization. As suggested in previous studies,[4,18] the large electron spin splitting in DMS[19] can be employed to fully polarize the 2D electron gas even at relatively low magnetic fields. Then, when only conduction-band Landau levels with one spin component ($j_e = -\frac{1}{2}$) are populated, one may expect clear evidence of electron-exchange interactions. Unusual magneto-optical features reported in the present study provide strong evidence of many-body effects in the spin-polarized 2DEG. We are able to clearly distinguish the many-body effects by using magnetic field to tune phase-space filling of particular Landau levels. None of the previous papers reported evidence of such effects in quantum structures. Despite the observation of inter-Landau-level transitions in Ref. 4, the Mn concentration ($x \leqslant 0.01$) was too low to polarize the 2D electron gas for integer filling factors $\nu \geqslant 2$, while in Ref. 18, many-body effects are not discussed.

II. SAMPLES AND EXPERIMENTAL SETUP

The magnetoabsorption measurements were performed on one-side modulation-doped $Cd_{1-x}Mn_xTe/Cd_{1-y}Mg_yTe$ heterostructures with a single 100 Å thick $Cd_{1-x}Mn_xTe$ QW grown by molecular beam epitaxy (MBE) on (001)-oriented GaAs substrates. The $Cd_{1-y}Mg_yTe$ buffer layer is transparent in the spectral region, corresponding to the fundamental interband transition in the QW. The iodine-doped region of 100 Å width was separated from the well by a 400 Å thick undoped barrier. The details of the growth procedure of $Cd_{1-x}Mn_xTe/Cd_{1-y}Mg_yTe$ MDQW's were published in Ref. 20.

In order to estimate the electron concentration n_e we performed magnetotransport measurements at 1.7 K. Magnetic

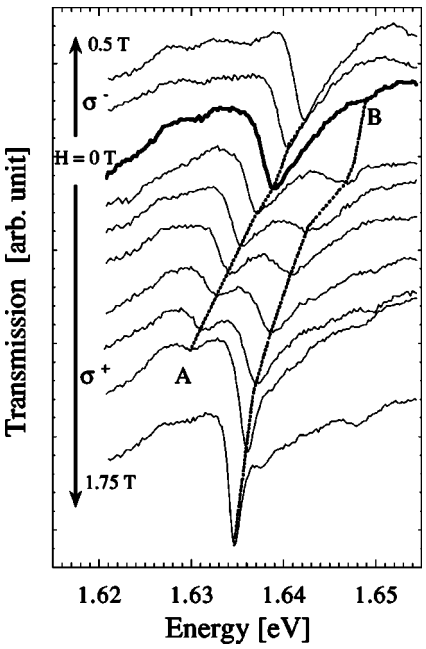

FIG. 1. Evolution of the transmission spectrum at low field in Faraday configuration with $\sigma^{\pm}$ polarization. The magnetic field increases with the step of 0.25 T between curves.

field values corresponding to integer filling factors deduced from Shubnikov–de Haas oscillations are presented with the magneto-optical data in Sec. III. Observations of cyclotron resonance by far-infrared magnetoabsorption lead to the determination of the electron effective mass $m_e/m_0=0.105$.

The magnetoabsorption experiments in the near-infrared region were carried out in the Faraday configuration, with the magnetic field applied parallel to the growth axis, in both σ^+ and σ^- circular polarizations at 1.7 K up to 7 T. Since several samples with slightly different compositions measured in our experiments gave qualitatively the same results, below we focus on just one of them. For this sample, the Mg concentration in the barriers was $y=0.147$. The Mn content within the QW, estimated from a calibration of molecular flux during the MBE growth, was $x\approx 0.02$.

Assuming the lattice parameter of the QW is set by the $Cd_{1-y}Mg_yTe$ buffer and barriers, it is possible to estimate the effect of the strain on the band-gap energy. For $x\approx 0.02$ and $y=0.147$, using the Mn and Mg concentration dependence of the lattice parameter[21,22] and the strain constants for CdTe,[23] the $HH_1\rightarrow E_1$ transition energy is predicted to increase by 0.3 meV. For magnetotransmission measurements, the GaAs opaque substrate was removed by chemical etching. This has no impact on the strain of the QW: reflectivity and transmission measurements performed, respectively, before and after etching of the substrate, give the same transition energies at zero field. From now on, strain effects will be neglected in our study.

III. EXPERIMENTAL RESULTS

The zero-field transmission spectrum consists of an asymmetrical line (A) at 1639.5 meV and a very weak feature (B) at 1649.5 meV (Fig. 1). At nonzero magnetic field, a large Zeeman effect is observed: the line (A) splits into a σ^--polarized high-energy component of a nearly constant

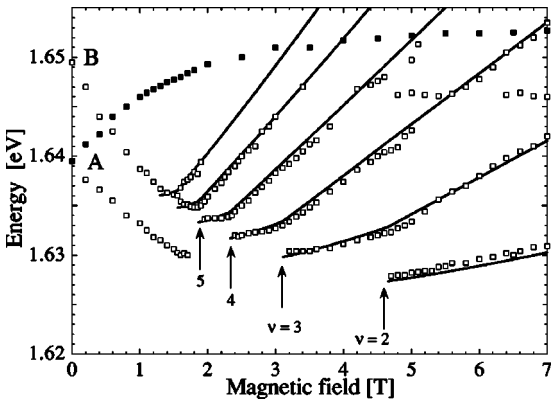

FIG. 2. Magnetic field dependence of the transition energies. Symbols: experiments (open symbols) σ^+, (closed symbols) σ^-. Solid lines: theoretical fit obtained for parameters $x=0.018$, $E_a^*=1644.5$ meV, $\hbar\omega^*/H=1.5$ meV/T, and $R_0=2.5$ meV. The integer filling factors are indicated by arrows.

intensity with a Zeeman shift nearly saturated at $H\sim 5$ T, and a σ^+-polarized low-energy component that weakens with increasing field and disappears at $H\sim 1.5$ T. In contrast, feature (B), hardly visible at zero field, gains intensity and evolves into a set of L_n lines visible in the σ^+ polarization. With increasing magnetic field the energies of L_n lines shift towards higher energies, as shown in Fig. 2.

We focus first our attention on the lines L_n that appear at discrete values of the field in σ^+ polarization. In order to follow the magnetic field evolution of the L_n lines, we have plotted in Fig. 3 several transmission spectra taken between 2.8 and 5.4 T in the σ^+ polarization. At $H=2.8$ T, two lines, labeled L_3 and L_4, can be observed. The energies of these lines [$E_3(H)$ and $E_4(H)$] increase with increasing magnetic field. At $H=3.1$ T, a new line, L_2, appears. The intensity of the L_2 line rapidly grows and at $H=3.4$ T it becomes comparable to the intensity of L_3. In this field range (3.1–3.4 T)

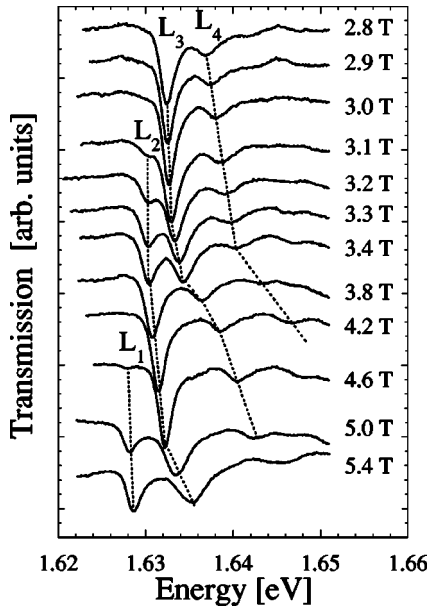

FIG. 3. Magnetotransmission spectra betwen 2.8 and 5.4 T (σ^+ polarization). The magnetic field increases with the step of 0.1 T (0.4 T) between 2.8 T and 3.4 T (3.4 T and 5.4 T).

the energy of the L_2 line remains independent of magnetic field ($E_2 = 1630.5$ meV) and starts to increase only at $H > 3.4$ T. At $H = 4.6$ T, when the intensity of the L_2 line reaches a maximum, a new line, L_1, emerges from the background on the low-energy side of the spectrum. Above 4.6 T, line L_1 is weakly shifted and intensified in the field while L_2 moves to higher energy and weakens. The same behavior is found for all observed transitions ($L_1, \ldots, L_6$) in the investigated field range.

The L_n lines, observed in the σ^+ polarization, display a similar behavior as the inter-Landau-level transitions between the HH_1 heavy-hole states with angular momentum $j_h = 3/2$ and the E_1 electron states with spin component $j_e = -1/2$ along the magnetic field. For interband transitions, the magnetic field dependence of the energies, $E_n(H)$, is

$$E_n(H) = E_a + (n + \tfrac{1}{2})\hbar\omega^* + E^{sp\text{-}d}(H), \qquad (1)$$

where E_a is the renormalized band gap[8] associated with the $HH_1 \rightarrow E_1$ transition, $\hbar\omega^* = \hbar eH/\mu c$ is the reduced cyclotron energy with the reduced mass μ ($1/\mu = 1/m_e + 1/m_h$; m_e and m_h are the in-plane effective masses of electron and hole, respectively). The $E^{sp\text{-}d}(H)$ term describes the spin-dependent contribution caused by the (sp-d) exchange interactions between localized spins of Mn ions and carriers. In the $Cd_xMn_{1-x}Te$ QW, the (sp-d) energy contributions for the $j_e = -1/2$ conduction-band edge and $j_h = 3/2$ valence-band edge are equal to $-\frac{1}{2}N_0\alpha x S_z$ and $-\frac{1}{2}N_0\beta x S_z$, respectively. $N_0\alpha$ and $N_0\beta$ denote the conduction and valence exchange integrals, x is the molar Mn fraction, and S_z is the mean value of the Mn spin in the direction of the external magnetic field. In the high-field region, where S_z is saturated ($H \geqslant 5$ T), the energies of L_n lines are well described by the diamagnetic term, $(n + \frac{1}{2})\hbar\omega^*$, with $n = 2$ and 3 for L_2 and L_3, respectively, using the values of the electron effective mass deduced from our cyclotron resonance measurements ($m_e/m_0 = 0.105$) and from the hole effective mass in CdTe ($m_h/m_0 = 0.193$).[24]

As shown in Fig. 2, every absorption line L_n appears at a discrete magnetic field, H_n when the $n_\downarrow$ electron Landau level reaches the Fermi level. At $H > H_n$, emptying states become available for optical excitation. The H_n values correspond then to the integer values of the electron filling factor, $\nu = n + 1$. As reported in Fig. 4, the inverse of magnetic field, H_n^{-1}, is proportional to $\nu = n + 1$, yielding the concentration of the 2DEG, n_e:

$$\frac{H_n^{-1}}{\nu} = \frac{e}{hcn_e}. \qquad (2)$$

The value $n_e = 2.25 \times 10^{11}$ cm^{-2} determined by the magneto-optical experiment is in excellent agreement with the results obtained from Shubnikov–de Haas measurements performed on the same sample (Fig. 4). It corresponds to a zero field electron Fermi energy, $E_F = \pi\hbar^2 n_e/m_e = 5.2$ meV. Note that the observation of the continuous sequence of integer filling factor $\nu = 2, \ldots, 6$ in the only σ^+ polarization, between 1.5 and 7 T, indicates the full spin polarization of the electron gas above $H = 1.5$ T.

In order to emphasize peculiarities visible in magnetic field dependencies of transition energies $E_n(H)$, we

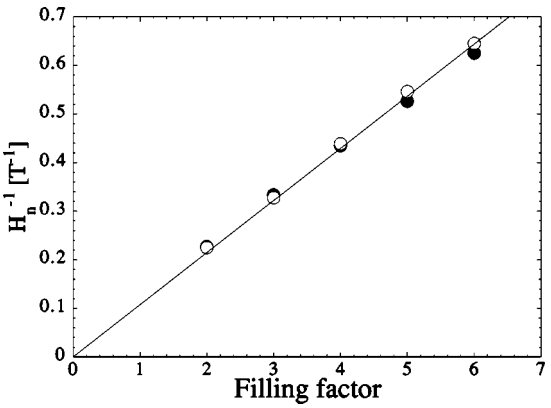

FIG. 4. Reciprocal magnetic field H_n^{-1} versus integer filling factors ν. Closed circles denote the field at which the lines L_n appear in transmission experiments. Open circles denote the position of the resistivity minima in Shubnikov–de Haas measurements.

plotted, in Fig. 5, the energy differences $\Delta_n(H) = E_{n+1}(H) - E_n(H)$ ($n \geqslant 1$) between consecutive lines L_{n+1} and L_n in a given field. This procedure eliminates the contribution caused by the sp-d exchange interaction. In the field region $H > H_{n-1}$ corresponding to $\nu \leqslant n$, all $\Delta_n(H)$ energy differences merge into an unique straight line of slope $\hbar\omega^*/H = 1.5 \pm 0.1$ meV/T, but the zero-field extrapolated energy δ is not zero: $\delta \approx 1$ meV. For each energy separation $\Delta_n(H)$ between adjacent lines L_n, one observes a break in the linear field dependence at field H_{n-1}, corresponding to $\nu = n$. Below H_{n-1}, the energies $\Delta_n(H)$ decrease sharply with decreasing H, reflecting a change of behavior of the line L_n.

The observed features show the existence of two regimes in the field dependence of the lines L_n depending on the occupancy of the $n_\downarrow$ Landau level: (1) in the region $H > H_{n-1}$ ($\nu < n$), the $n_\downarrow$ Landau level is empty and the energy of the line L_n varies linearly with H through the diamagnetic term $(n + \frac{1}{2})\hbar\omega^*$, as expected for inter-Landau-level transitions. (2) In the region $H_n < H < H_{n-1}$ ($n < \nu < n + 1$), the $n_\downarrow$ Landau level is partially occupied and the energies $E_n(H)$ of the line L_n display a much weaker field dependence than that

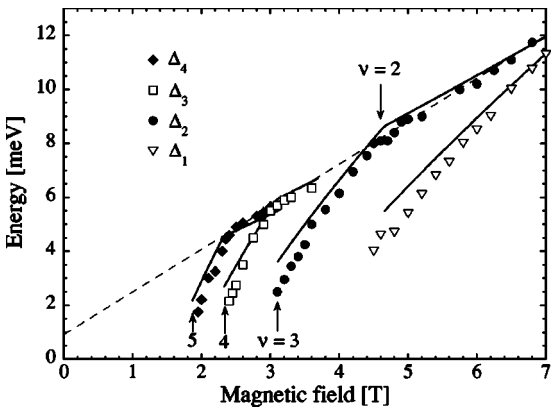

FIG. 5. Energy difference $\Delta_n = E_{n+1} - E_n$ between consecutive lines L_n versus magnetic field. Symbols: experiments. Solid lines: theoretical fit obtained for $\hbar\omega^*/H = 1.5$ meV/T and $R_0 = 2.5$ meV. The integer filling factors are indicated by arrows. The slope of the dashed line is 1.5 meV/T.

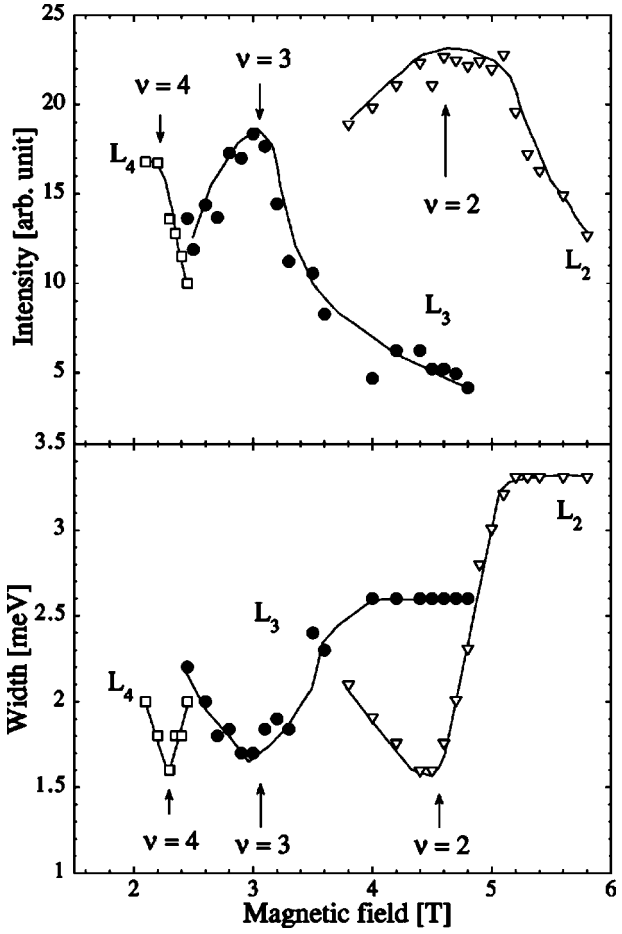

FIG. 6. Magnetic field dependence of the intensity (a) and width (b) of line L_n ($2 \leqslant n \leqslant 4$).

expected for interband transitions. These effects are also visible in the transmission spectra (Fig. 3) and in the fan chart (Fig. 2).

An additional proof for the existence of the two regimes ($\nu < n$ and $\nu > n$) is provided by an analysis of the magnetic field dependence of intensities and widths of the L_n absorption lines. As shown in Fig. 6(a), the intensity of each transition line increases at low fields reaches a maximum at $\nu = n$ and decreases in the high-field region where $\nu < n$. The opposite effect is found for the transition linewidth. It shows a minimum for $\nu = n$ [Fig. 6(b)]. Such a change of behavior of the energies and strengths of the magneto-optical transitions at $\nu = n$ has been predicted theoretically by Bauer[25] for a 100 Å $GaAs/Ga_xAl_{1-x}As$ MDQW with an electron density $n_e = 1.2 \times 10^{11}$ cm^{-2} at $T = 0.5$ K.

The following conclusions can be drawn from experimental data:

(1) The sequence of lines L_n, periodic in $\hbar\omega^*$ at $H > H_{n-1}$, results from the excitation of electron-hole pairs between HH_1 and E_1 Landau levels. The e-h Coulomb interaction has to be taken into account to explain the finite value of δ. In the region $H_n < H < H_{n-1}$, the transition $n \rightarrow n$ are strongly affected by the phase-space filling of the nth electron Landau level.

(2) The very weak structure (B) observed at 1649.5 meV at zero field follows the magnetic field dependence of the onset of the line L_n (Fig. 2). Structure (B) could be attributed to the Moss-Burstein edge of the $HH_1 \rightarrow E_1$ interband transitions at $E_a + E_F(1 + m_e/m_h)$. The $HH_1 \rightarrow E_1$ energy gap $E_a = 1641.6 \pm 0.5$ meV is deduced from the Fermi energy ($E_F = 5.2$ meV) and from the effective masses.

(3) In the region $H < 1.5$ T where both spin states $j_e = \pm\frac{1}{2}$ are populated, negatively charged excitons (trions) can be formed. We assign the line (A) observed below 1.5 T to the X^- trion transition. Since the spin-down electron states are always populated, the high-energy trion state, formed of $(j_h = -\frac{3}{2}, j_e = \frac{1}{2})$ photocreated exciton and $(j_e = -\frac{1}{2})$ electron states, is observed in σ^- polarization at any magnetic field. In contrast, the spin-up states become empty at about $H = 1.5$ T, and the low-energy component of line (A), i.e., the $(j_h = \frac{3}{2}, j_e = -\frac{1}{2})(j_e = \frac{1}{2})$ trion state vanishes with increasing field, as shown in Fig. 2 in the σ^+ polarization.

At zero field, the line (A) is found at 1639.5 meV in the doped quantum well. As shown in different studies,[14,4] the energy of the lowest excitation (X^- in our case) is almost independent of the carrier density. One may thus estimate the manganese concentration from the free-exciton energy (E_X) expected for an undoped QW of identical characteristics, taking $E_{b1} = 2.1$ meV for the X^- binding energy. The energy value $E_X = 1641.6$ meV corresponds to a $Cd_xMn_{1-x}Te$ QW of Mn composition $x = 0.018$. From now on, we will assign to the $Cd_xMn_{1-x}Te$ QW this value of the Mn composition. For $x = 0.018$, the expected exciton Zeeman shift due to the Mn-carrier exchange interaction is $E^{sp\text{-}d} = 19$ meV in the saturation region. However, the position of lines L_2 and L_3 in the saturation region implies a much larger spin contribution (≈ 27–28 meV) to satisfy Eq. (1) with the energies $E_a = 1641.6$ meV and $\hbar\omega^*/H = 1.5 \pm 0.1$ meV/T. This apparent contradiction between the values of $E^{sp\text{-}d}$ is in fact the manifestation of an *enhanced spin splitting* in the doped QW resulting from the electron-exchange interaction. We show in Sec. V that the overall experimental transitions can be quantitatively explained when taking into account the electron-exchange interaction and the e-h Coulomb interaction for a $Cd_xMn_{1-x}Te$ QW of $x = 0.018$.

IV. MODEL

To explain the observed behavior, we use a simplified model in the high-field approximation: We assume that the Coulomb interaction between photocreated electron and hole issued from E_1 and HH_1 Landau levels is weaker than the reduced cyclotron energy $\hbar\omega^*$. We determine the binding energy of the e-h pair associated with each inter-Landau-level transition by first-order perturbation theory. We also include the exchange energy of conduction electrons due to the 2D electron gas. The validity of this high-field approximation is justified from the parameters obtained by comparison with experimental data.

We consider a 2D system. In the effective mass approximation, in presence of a magnetic field $\mathbf{H}$ and e-h Coulomb interaction, the Hamiltonian of the e-h pair is ($e > 0$)

$$\mathcal{H} = \frac{(\mathbf{p}_e + e\mathbf{A}(\mathbf{r}_e)/c)^2}{2m_e} + \frac{(\mathbf{p}_h - e\mathbf{A}(\mathbf{r}_h)/c)^2}{2m_h} - \frac{e^2}{\kappa|\mathbf{r}_e - \mathbf{r}_h|}. \quad (3)$$

$\mathbf{A}(\mathbf{r}) = \frac{1}{2}\mathbf{H} \times \mathbf{r}$ is the potential vector; $\mathbf{r}_e$ and $\mathbf{r}_h$ are the electron and hole coordinates; $\mathbf{H}$ is perpendicular to the 2D QW;

κ is an effective dielectric constant including the effect of screening on the reduction of Coulomb interaction.

We consider the coordinates system $(\mathbf{R},\mathbf{r})$ defined by

$$\mathbf{R}=\frac{m_e\mathbf{r}_e+m_h\mathbf{r}_h}{m_e+m_h},$$
$$\mathbf{r}=\mathbf{r}_e-\mathbf{r}_h. \tag{4}$$

In the absence of a Coulomb interaction, the eigenfunctions of $\mathcal{H}$, $\Phi(\mathbf{r},\mathbf{R})$, can be written as

$$\Phi(\mathbf{r},\mathbf{R})=\frac{1}{\sqrt{S}}e^{i\mathbf{K}\cdot\mathbf{R}}e^{ie\mathbf{A}(\mathbf{r})\cdot\mathbf{R}/\hbar c}\Psi^{\mathbf{K}}_{n,m}(\mathbf{r}), \tag{5}$$

where S is the sample area, $\mathbf{K}$ is the total e-h momentum, and $\Psi^{\mathbf{K}}_{n,m}(\mathbf{r})$ (n,m integer $\geqslant 0$) is eigenfunction of

$$\mathcal{H}_1=\frac{\hbar^2K^2}{2M}+2\frac{\hbar e}{Mc}\mathbf{K}\cdot\mathbf{A}(\mathbf{r})-\frac{\hbar^2}{2\mu}\Delta-\frac{i\hbar e}{2c}\left(\frac{1}{m_e}-\frac{1}{m_h}\right)H\frac{\partial}{\partial\phi}$$
$$+\frac{e^2}{8\mu c^2}H^2r^2-\frac{e^2}{\kappa r}, \tag{6}$$

with $M=m_e+m_h$.

In Faraday geometry $\mathbf{K}=\mathbf{0}$, and the e-h angular momentum conservation implies $l=n-m=0$. The allowed e-h pairs are the states $\Phi_n(\mathbf{r},\mathbf{R})$ associated with[26]

$$\Psi^0_{n,n}(\mathbf{r},\mathbf{R})=(-1)^n\frac{e^{-r^2/4l_c^2}}{\sqrt{2\pi l_c^2}}L_n^0\left(\frac{r^2}{2l_c^2}\right), \tag{7}$$

with the energies $\epsilon_{nn}=(n+\frac{1}{2})\hbar\omega^*$. $L_n^m(x)$ are Laguerre polynomials[27] and $l_c=(\hbar c/eH)^{1/2}$ is the magnetic length.

Including the e-h Coulomb interaction, in the absence of electron gas, the binding energy of the e-h pair associated with the nth quantized state obtained from first-order perturbation theory is[26]

$$E_n^0(H)=\left\langle\Psi^{\mathbf{0}}_{n,n}\left|\frac{e^2}{\kappa r}\right|\Psi^{\mathbf{0}}_{n,n}\right\rangle=\sqrt{\frac{\pi}{2}}\frac{e^2}{\kappa l_c}C_{nn}=R_0\frac{a_0}{l_c}\sqrt{2\pi}C_{nn}, \tag{8}$$

where R_0 and a_0 are effective parameters defined by $R_0=\mu e^4/2\kappa^2\hbar^2$ and $a_0=\hbar^2\kappa/\mu e^2$. The coefficients $C_{nn'}$ are given by

$$C_{nn'}=\frac{2}{\sqrt{\pi}}\int_0^{+\infty}dx\,e^{-x^2}L_n^0(x^2)L_{n'}^0(x^2). \tag{9}$$

In the presence of an electron gas, we consider the state $\nu=(n+1)^-$ (as discussed in Ref. 28), with only one empty state in the conduction Landau level n. After creation of an e-h pair, the Landau level n is fully occupied. It is not possible to minimize the energy of the photocreated e-h pair by coupling this pair with other allowed pairs issued from the Landau level n. The binding energy is zero: $E_n^b(H_n)=0$.

In the intermediate regime, $n<\nu<n+1$, when the Landau level n is partially occupied, we assume that the e-h binding energy follows the relation (reproducing the two limiting cases previously discussed):

$$E_n^b(H)=E_n^0(H)(1-\tau_n), \tag{10}$$

with τ_n the filling factor of level $n(0\leqslant\tau_n\leqslant 1)$. When τ_n decreases, the phase-space filling is reduced; the number of allowed e-h pair excitations increases, which permit us to minimize on a larger subspace the ground-state energy, thus increasing the binding energy.

We consider now the exchange energy of the conduction electrons, distributed over Landau levels n'. In the 2D limit, the exchange energy has been derived by Ando and Uemura[29] and more recently by MacDonald *et al.*[30] in the presence of magnetic field. For an electron on Landau level n (and spin σ), the exchange energy $E^{exch}_{n,\sigma}(H)$ is

$$E^{exch}_{n,\sigma}(H)=-\frac{e^2}{\kappa l_c}\sqrt{\frac{\pi}{2}}\sum_{n'}\tau_{n'\sigma}C_{n,n'}$$
$$=-R_0\frac{a_0}{l_c}\sqrt{2\pi}\sum_{n'}\tau_{n'\sigma}C_{n,n'}, \tag{11}$$

where $\tau_{n'\sigma}$ is the filling factor of conduction Landau level n' of spin σ. In our case, we consider only electrons with spin-down component as the electron gas is polarized ($H\geqslant 1.5$ T). The exchange energy is zero for spin-up conduction electrons.

V. ANALYSIS AND DISCUSSION

In order to describe the magnetic field dependence of $E_n(H)$, one has to take into account the energy terms originating from electron-hole Coulomb and the electron-exchange interactions. According to the high-field approximation described above, the following formula has to be employed instead of Eq. (1):

$$E_n(H)=E_a^*+(n+\tfrac{1}{2})\hbar\omega^*+E^{sp\text{-}d}(H)+E_n^{exch}(H)-E_n^b(H), \tag{12}$$

where $E_n^{exch}(H)$ and $E_n^b(H)$ are the exchange energy experienced by an electron in the $n_\downarrow$ Landau level and the e-h binding energy, respectively. $E_a^*=E_a-E^{exch}(0)$ is the $HH_1\rightarrow E_1$ energy gap, after subtracting the zero-field exchange energy that is already included in the fourth term of Eq. (12).

Comparison with experiment is achieved using a two-step procedure and taking advantage of the fact that the energy differencies $\Delta_n(H)$ between consecutive L_n transitions are *independent of the spin splitting* $E^{sp\text{-}d}(H)$, as follows.

(i) The energy difference $\Delta_n(H)$ between consecutive lines

$$\Delta_n(H)=\hbar\omega^*+[E_n^b(H)-E_{n+1}^b(H)]$$
$$+[E_{n+1}^{exch}(H)-E_n^{exch}(H)] \tag{13}$$

depends only on two parameters, the reduced cyclotron energy $\hbar\omega^*$ and R_0. The solid lines plotted in Fig. 5 result from this first step of the fitting procedure. For $\nu<n$, the experimental points gather on a single line the slope of which, $\hbar\omega^*/H=1.5\pm 0.1$ meV/T, determines the cyclotron energy. In the low-field regime ($n\leqslant\nu\leqslant n+1$), the slope of $\Delta_n(H)$ (calculated for $R_0=2.5$ meV) accounts for the

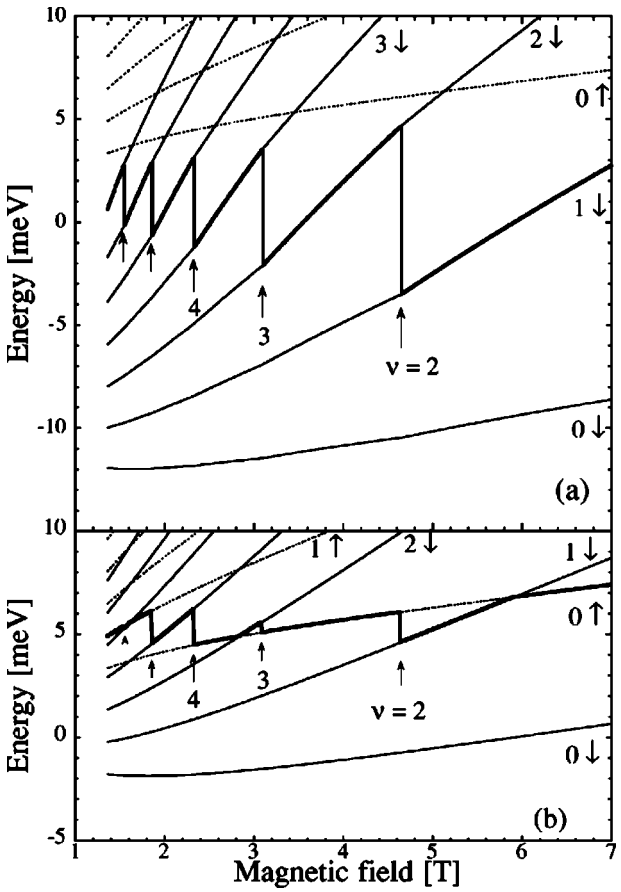

FIG. 7. Energies of conduction Landau levels versus magnetic field for both spin components: $n_\uparrow$ (dashed lines) and $n_\downarrow$ (solid lines). The Fermi energy is represented by a thick line. (a) Calculated from the model including electron-exchange interaction, for parameters $x=0.018$ and $m_e/m_0=0.105$. (b) In the absence of exchange interaction for the same parameters.

field dependence of all experimental energy differences $\Delta_n(H)(1\leqslant n\leqslant 4)$ with an accuracy better than 1 meV.

Note that, in the absence of Coulomb interactions, $\Delta_n(H)$ is equal to $\hbar\omega^*$. In such a case all $\Delta_n(H)$ would gather on a single line that extrapolates to the origin. The finite value of $\delta\approx 1$ meV and the existence of two distinct regimes for each curves $\Delta_n(H)$ is the signature of the Coulomb interaction and the phase-space-filling effect.

(ii) Energies $E_n(H)$ of the lines L_n are fitted to the experimental spectra, taking as a free parameter E_a^*. Other parameters are fixed: $\hbar\omega^*/H=1.5$ meV/T, $R_0=2.5$ meV, and $x=0.018$. $E^{sp\text{-}d}(H)$ denotes the spin contribution originating from Mn-carrier exchange interaction. $E^{sp\text{-}d}(H)$ is calculated using the expression of S_z versus x and H, given by Grieshaber *et al.*[31] and deduced from their study of the bulk alloy Zeeman splitting. The best fits, shown in Fig. 2, are achieved for $E_a^*=E_a-E^{exch}(0)=1644.5\pm 1$ meV. Excellent agreement is found between the transition energies calculated from the model and the experimental positions of the lines L_n $(1\leqslant n\leqslant 6)$, between 1.5 and 7 T, with an accuracy better than 0.5 meV. The value of the zero-field energy $E_a^*=1644.5\pm 1$ meV is quite consistent with the value of $E_a=1641.6\pm 0.5$ meV deduced from the position of structure (*B*) at the Moss-Burstein edge and with the zero-field exchange energy $E^{exch}(0)=-3.9$ meV, calculated from the relation[32]

$$E^{exch}(0)=-R_0a_0\frac{8}{3}\sqrt{\frac{2n_e}{\pi}}. \tag{14}$$

Thus, one may estimate the band-gap renormalization (BGR) induced by the electron gas: for an undoped $Cd_{1-x}Mn_xTe$ QW of identical characteristics ($L=100$ Å, $x=0.018$), the $HH_1\rightarrow E_1$ transition energy should lie at 1661 meV, while we obtain $E_a=1641.5$ meV for the doped QW. The BGR deduced from our analysis, approximately 20 meV, is in good agreement with the values given in $Cd_xMn_{1-x}Te$ MDQW for the concentration range $n_e=(2-4.8)\times 10^{11}$ cm^{-2}.[4]

In doped semiconductors, the band gap is renormalized by many-body effects caused by the presence of free carriers. E_a is then the band gap renormalized by exchange-correlation effects, in presence of electron-phonon coupling.[33,34] We assume that the main magnetic field dependence of the renormalization is in the exchange correction, which is sensitive to the spin populations. Within this assumption, it was possible to introduce in our analysis the energy E_a^*, which includes all the renormalization corrections except exchange.

As we mentioned in Sec. III, there is an apparent contradiction between the Zeeman shift expected for Mn content of $x=0.018$ and that observed in the experiment. In order to understand this effect, we plot, in Fig. 7, the scheme of conduction electron Landau levels obtained for $x=0.018$ and $m_e/m_0=0.105$. In Fig. 7(a) the exchange terms are included into calculations, while in Fig. 7(b) we neglect them. The exchange interactions drastically enhance the Landau-level spin splitting. The combined effects of Mn-electron and electron-exchange interactions lead to the complete spin polarization of the electron gas in the considered field range.

VI. CONCLUSIONS

The present study emphasizes the strong influence of the many-body exchange interactions on the Landau-level spin states. The overall experimental transitions observed in the magnetotransmission experiments are consistently interpreted in the frame of a simple model based on the high-field approximation. The validity of the basis assumption ($E_n^0<\hbar\omega^*$) was confirmed by the comparison of parameters deduced from model with experimental ones. The ratio η of the first-order correction $E_n^0(H)$ to the Landau splitting $\hbar\omega^*$ is $\eta=C_{nn}\sqrt{(\pi R_0/\hbar\omega^*)}$. The value of $\eta=C_{nn}\sqrt{n}\sqrt{\mu R_0/2n_e\hbar^2}$ at $\nu=n$ varies for the different transitions between 0.67 (for $n=1$) and 0.84 (for $n=6$), and this ratio decreases for each transition with increasing magnetic field.

ACKNOWLEDGMENTS

The authors want to thank J.-P.Vieren for making FIR magnetotransmission and magnetotransport measurements. This work was partially supported by Committee for Scientific Research (Poland) under Grant No. 2P03B 119 14.

[1] K. Kheng, R. T. Cox, Y. Merle d'Aubigné, F. Bassani, K. Saminadayar, and S. Tatarenko, Phys. Rev. Lett. **71**, 1752 (1993).
[2] G. Finkelstein, H. Shtrikman, and I. Bar-Joseph, Phys. Rev. Lett. **74**, 976 (1995).
[3] D. R. Yakovlev, V. P. Kochereshko, R. A. Suris, H. Schenk, W. Ossau, A. Waag, G. Landwehr, P. C. M. Christianen, and J. C. Maan, Phys. Rev. Lett. **79**, 3974 (1997).
[4] T. Wojtowicz, M. Kutrowski, G. Karczewski, J. Kossut, F. Teran, and M. Potemski, Phys. Rev. B **59**, R10 437 (1999).
[5] G. Finkelstein, H. Shtrikman, and I. Bar-Joseph, Phys. Rev. B **53**, 12 593 (1996).
[6] C. Delalande, G. Bastard, J. Orgonasi, J. A. Brum, H. W. Liu, M. Voos, G. Weimann, and W. Schlapp, Phys. Rev. Lett. **59**, 2690 (1987).
[7] D. A. Kleinman, Phys. Rev. B **32**, 3766 (1985).
[8] S. Schmitt-Rink, D. S. Chemla, and D. A. B. Miller, Adv. Phys. **38**, 89 (1989).
[9] A. E. Ruckenstein and S. Schmitt-Rink, Phys. Rev. B **35**, 7551 (1987).
[10] G. D. Sanders and Y.-C. Chang, Phys. Rev. B **35**, 1300 (1987).
[11] M. Kemerink, P. M. Koenraad, P. C. M. Christianen, R. van Schajk, J. C. Maan, and J. H. Wolter, Phys. Rev. B **56**, 4853 (1997).
[12] P. Kossacki, J. Cibert, D. Ferrand, Y. Merle d'Aubigné, A. Arnoult, A. Wasiela, S. Tatarenko, and J. A. Gaj, Phys. Rev. B **60**, 16 018 (1999).
[13] T. Wojtowicz, M. Kutrowski, G. Karcewski, and J. Kossut, Appl. Phys. Lett. **73**, 1379 (1998).
[14] V. Huard, R. T. Cox, K. Saminadayar, A. Arnoult, and S. Tatarenko, Phys. Rev. Lett. **84**, 187 (2000).
[15] R. T. Cox *et al.*, in *Proceedings of the 11th International Conference on High Magnetic Field in the Physics of Semiconductors*, edited by D. Heiman (World Scientific, Singapore, 1994).
[16] S. Takeyama, G. Karczewski, T. Wojtowicz, J. Kossut, H. Kunimatsu, K. Uchida, and N. Miura, Phys. Rev. B **59**, 7327 (1999).
[17] F. J. Teran, M. L. Sadowski, M. Potemski, G. Karczewski, S. Maćkowski, and J. Jaroszyński, Physica B **258**, 577 (1998).
[18] S. A. Crooker, D. G. Rickel, I. P. Smorchkova, N. Samarth, J. M. Kikkawa, and D. D. Awschalom, J. Appl. Phys. **85**, 5932 (1999).
[19] J. A. Gaj, R. Planel, and G. Fishman, Solid State Commun. **29**, 435 (1979).
[20] G. Karczewski, J. Jaroszyński, A. Barcz, M. Kutrowski, T. Wojtowicz, and J. Kossut, J. Cryst. Growth **184/185**, 814 (1998).
[21] W. Giriat and J. K. Furdyna, *Semiconductors and Semimetals*, edited by J. K. Furdyna and J. Kossut (Academic, London, 1988), Vol. 25, p. 275.
[22] J. M. Hartmann, J. Cibert, F. Kany, H. Mariette, M. Charleux, P. Alleysson, R. Langer, and G. Feuillet, Appl. Phys. Lett. **80**, 6257 (1996).
[23] Y. Merle d'Aubigné, H. Mariette, N. Magnea, H. Tuffigo, R. T. Cox, G. Lentz, Le Si Dang, J.-L. Pautrat, and A. Wasiela, J. Cryst. Growth **101**, 650 (1990).
[24] C. Neumann, A. Nöthe, and N. O. Lipari, Phys. Rev. B **37**, 922 (1988).
[25] G. E. W. Bauer, Solid State Commun. **78**, 163 (1991).
[26] A. H. MacDonald and D. S. Ritchie, Phys. Rev. B **33**, 8336 (1986).
[27] I. S. Gradshteyn and I. M. Ryzhik, *Tables of Integrals, Series, and Products* (Academic Press, London, 1965).
[28] P. Hawrylak and M. Potemski, Phys. Rev. B **56**, 12 386 (1997).
[29] T. Ando and Y. Uemura, J. Phys. Soc. Jpn. **37**, 1044 (1974).
[30] A. H. MacDonald, H. C. A. Oji, and K. L. Liu, Phys. Rev. B **34**, 2681 (1986).
[31] W. Grieshaber, A. Haury, J. Cibert, Y. Merle d'Aubigné, A. Wasiela, and J. A. Gaj, Phys. Rev. B **53**, 4891 (1996).
[32] F. Stern, Phys. Rev. Lett. **30**, 278 (1973).
[33] S. Das Sarma, R. Jalabert, and S.-R. Eric Yang, Phys. Rev. B **39**, 5516 (1989).
[34] R. Jalabert and S. Das Sarma, Phys. Rev. B **40**, 9723 (1989).